

O-band InAs/GaAs quantum-dot microcavity laser on Si (001) hollow substrate by *in-situ* hybrid epitaxy

Cite as: AIP Advances 9, 015331 (2019); <https://doi.org/10.1063/1.5065527>

Submitted: 10 October 2018 . Accepted: 21 January 2019 . Published Online: 30 January 2019

Bin Zhang, Wen-Qi Wei, Jian-Huan Wang, Hai-Ling Wang , Zhuang Zhao, Lei Liu, Hui Cong, Qi Feng, Huiyun Liu, Ting Wang, and Jian-Jun Zhang



View Online



Export Citation



CrossMark

ARTICLES YOU MAY BE INTERESTED IN

[1.5 \$\mu\text{m}\$ quantum-dot diode lasers directly grown on CMOS-standard \(001\) silicon](#)

Applied Physics Letters **113**, 221103 (2018); <https://doi.org/10.1063/1.5055803>

[Perspective: The future of quantum dot photonic integrated circuits](#)

APL Photonics **3**, 030901 (2018); <https://doi.org/10.1063/1.5021345>

[Semiconductor quantum dot lasers epitaxially grown on silicon with low linewidth enhancement factor](#)

Applied Physics Letters **112**, 251111 (2018); <https://doi.org/10.1063/1.5025879>

Don't let your writing
keep you from getting
published!

AIP | Author Services

Learn more today!

O-band InAs/GaAs quantum-dot microcavity laser on Si (001) hollow substrate by *in-situ* hybrid epitaxy

Cite as: AIP Advances 9, 015331 (2019); doi: 10.1063/1.5065527

Submitted: 10 October 2018 • Accepted: 21 January 2019 •

Published Online: 30 January 2019



Bin Zhang,^{1,2,3} Wen-Qi Wei,¹ Jian-Huan Wang,^{1,2} Hai-Ling Wang,^{1,3}  Zhuang Zhao,⁴ Lei Liu,⁴ Hui Cong,¹ Qi Feng,¹ Huiyun Liu,⁵ Ting Wang,^{1,2,a)} and Jian-Jun Zhang^{1,2,a)}

AFFILIATIONS

¹Beijing National Laboratory for Condensed Matter Physics, Institute of Physics, Chinese Academy of Sciences, Beijing 100190, China

²Center of Materials Science and Optoelectronics Engineering, University of Chinese Academy of Sciences, Beijing 100049, China

³School of Physical Sciences, University of Chinese Academy of Sciences, Beijing 100190, China

⁴Optical and Microwave Technology Research Department, Huawei Technologies Co., Ltd., Shenzhen 518129, China

⁵Department of Electronic and Electrical Engineering, University College London, London WC1E 7JE, UK

^{a)}Electronic mail: wangting@iphy.ac.cn; jjzhang@iphy.ac.cn

ABSTRACT

Recent years, the emergence of hyper-scale data centers boosted the research field of integrated silicon photonics. One of the major challenges for compact photonic integrated circuits is silicon based lasers. In this paper, we demonstrate optically pumped InAs/GaAs quantum-dot micropillar laser on exact Si (001) by (111)-faceted-sawtooth Si hollow structure via IV/III-V hybrid epitaxy. The lasing threshold of InAs/GaAs quantum-dot micropillar is as low as 20 μ W with the pillar diameter of 15 μ m. Moreover, the micropillar laser is capable of operating at maximum temperature up to 100 °C.

© 2019 Author(s). All article content, except where otherwise noted, is licensed under a Creative Commons Attribution (CC BY) license (<http://creativecommons.org/licenses/by/4.0/>). <https://doi.org/10.1063/1.5065527>

I. INTRODUCTION

Over the past decade, CMOS compatible III-V/Si hybrid light sources have been extensively explored for applications of silicon photonic integrated circuits.¹⁻³ At current stage, there are two major approaches, which are wafer (flip-chip) bonding techniques⁴⁻⁶ and direct epitaxial growth of III-V photonic devices on Si.⁶⁻¹⁰ Both of these techniques have their own pros and cons. The III-V/Si bonding methods exhibit outstanding device performance and lifetime, but generally have scalability, yield and cost issues. In contrast, the direct growth method can overcome scalability and yield issues, but encounters crystal quality problems, such as threading dislocations (TDs), antiphase boundaries (APBs) and micro thermal cracks, which are generally induced from the lattice mismatch, polarity difference and thermodynamic contrast between III-V

compounds and Si. Therefore, there are many researches carried on monolithic growth of InAs/GaAs quantum-dot (QD) lasers on Si substrates in last few years,¹¹⁻¹³ including techniques such as offcut Si (001) substrates,^{7,14} Ge/Si virtual substrates,^{15,16} hydrogen annealing process,^{8,17} intermediate GaP buffer¹⁸⁻²⁰ and V-grooved Si substrates.²¹⁻²⁴ However, most of above techniques suffer from high defect density and thermal mismatch induced material degradation. We have recently reported a CMOS compatible technique for achieving high-quality III-V layers on Si via homo-epitaxially grown (111)-faceted Si hollow structures by *in-situ* hybrid epitaxy.²⁵ In this work, optically pumped InAs/GaAs micropillar laser on such on-axis Si (001) substrate is fabricated and characterized. The InAs/GaAs micropillar laser on Si (001) exhibits a sub-milliwatt threshold pump power and maximum operating temperature up to 100 °C.

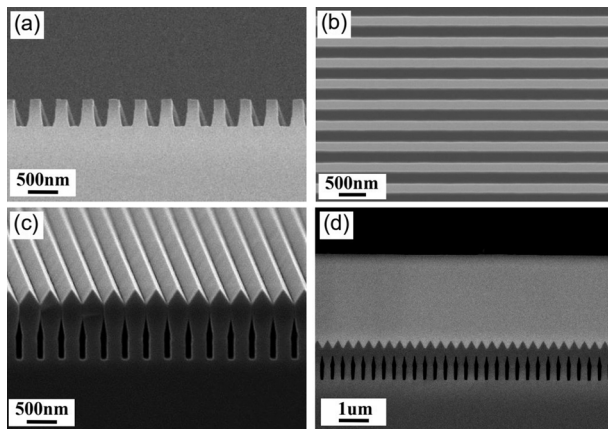


FIG. 1. (a), (b) Cross-sectional and top-view SEM images of U-shape patterned Si (001) substrates, respectively. (c) SEM image of (111)-faceted-sawtooth structure after 500 nm Si buffer on U-shape patterned Si (001). (d) Cross-sectional SEM image of GaAs buffer layers on (111)-faceted Si hollow structure.

II. MATERIAL GROWTH AND DEVICE FABRICATION

We implemented a heterostructure hybrid epitaxial method²⁵ to achieve a CMOS compatible platform for III-V microcavity lasers on exact Si (001) substrates. An 8-inch U-shape patterned Si (001) substrate is firstly prepared with CMOS-compatible deep ultraviolet (DUV) photolithography (180 nm feature size) and dry etching techniques. All patterning processes are completed over a CMOS process foundry, while the material growths are carried out in an III-V/IV dual chamber MBE system. Figure 1(a) shows the cross-sectional scanning electron microscope (SEM) image of Si U-shape structure, taken along [1-10] direction. The U-shape structure has a 360 nm period with 140 nm wide ridges and 480 nm in depth. The ridges lie along [110] direction, as the top-view SEM shows in Figure 1(b). Before loading into MBE chamber, the U-shape patterned Si substrates are cleaved into 32 mm by 32 mm for *in-situ* III-V/IV hybrid growth. By homo-epitaxial growth of a 500 nm silicon buffer layer on the U-shape

patterned substrate, highly uniform (111)-faceted-sawtooth hollow structure is obtained, as shown in the tilted SEM image of Figure 1(c). The GaAs film is grown by using a two-step method, which consists an AlAs nucleation layer at 380 °C and a high-temperature GaAs buffer layer at 560 °C. Subsequently, two types of dislocation filter layers (DFLs) are grown at 480 °C, including InGaAs/GaAs and InAlAs/GaAs multiple quantum wells (QWs). The APBs and most of the mismatch dislocations are confined and annihilated at the interface between the GaAs and the (111) faceted Si (001). The DFLs are utilized to further suppress the propagation of threading dislocations (TDs).¹⁹ At last, five periods of GaAs/Al_{0.6}Ga_{0.4}As superlattices (SLs) are deposited to smooth the surface. Figure 1(d) shows the cross-sectional SEM image of the entire buffer structures, indicating a high-quality GaAs film grown on (111)-faceted Si (001) substrate. To note, the detailed information related to material growth mechanism has been previously discussed in Ref. 25.

Figure 2(a) shows the schematic diagram of micropillar laser structure grown on GaAs/Si (001) substrate. The corresponding cross-sectional SEM image of such structure is shown in Figure 2(b), consisting of distributed Bragg reflectors (DBRs) and an active layer. The DBRs are made of 33.5 bottom and 15 top pairs of quarter-wavelength thick alternating GaAs/AlAs layers. The active layer in the center of one λ -thick GaAs cavity is sandwiched between top and bottom DBRs. Each repeat of AlAs/GaAs DBR includes 111.1 nm AlAs and 94.2 nm GaAs, grown at optimum temperature of 610 °C and 560 °C, respectively. The active layer contains five periods of InAs/GaAs dot-in-a-well (DWELLs) structure.¹⁵ Each period consists of a 3.1-monolayer InAs QD layer sandwiched by 2-nm In_{0.143}Ga_{0.857}As wetting layer and 6-nm In_{0.143}Al_{0.857}As capping layer, all grown at 450 °C. The InAs/GaAs QD micropillar laser structures on Si (001) were fabricated with diameters ranging from 15 μ m to 250 μ m, as shown in Figure 2(c). The scanning electron microscope (SEM) image of micropillar laser with 15 μ m diameter (Figure 2(d)) reveals the reasonably smooth cavity surface and sidewall. In this example, the etching depth reached down to the last 7-8 GaAs/AlAs mirror pairs of the bottom DBR.

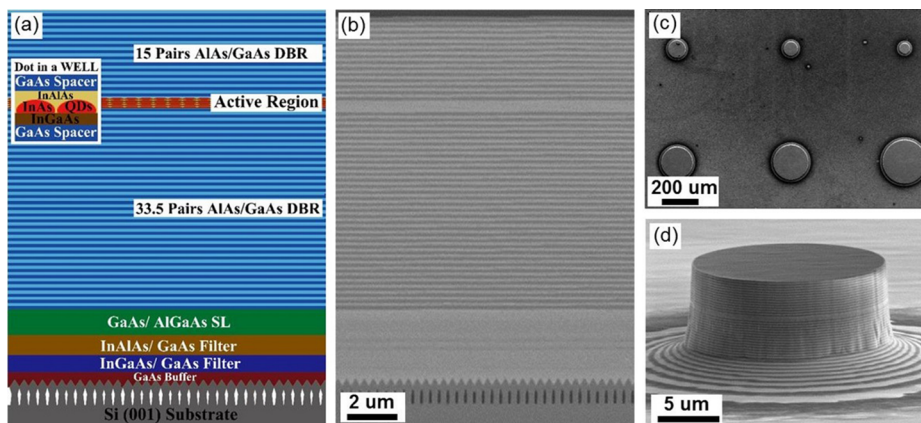


FIG. 2. The schematic diagram (a) and cross-sectional SEM image (b) of InAs/GaAs micropillar laser structure on (111)-faceted-sawtooth Si (001) hollow substrate: InAs/GaAs QDs embedded in one λ -cavity with 15 (33.5) pairs of top (bottom) DBRs; (c) top-view SEM image of micropillar lasers with different diameters; (d) SEM image of InAs/GaAs QD micropillar laser on Si (001) with 15 μ m diameter.

III. RESULTS AND DISCUSSION

By implementing the growth technique above, high quality GaAs buffer layer with a root-mean-square (RMS) roughness of approximately 0.4 nm across atomic force microscopy (AFM) scanning area of $2 \times 2 \mu\text{m}^2$ is achieved, as shown in Figure 3(b). The defect density of this GaAs/Si structure is estimated to be approximately in the range of 10^5 - 10^6 cm^{-2} by etch pit density (EPD) and electron channeling contrast image (ECCI) measurements, which is lowest reported up to date. In order to verify the influence of (111)-faceted-sawtooth Si (001) hollow structure on defect suppression at GaAs/Si interface, surface SEM images of identical GaAs structures directly grown on standard Si (left side of Figure 3(a)) and (111)-faceted-sawtooth Si (right side of Figure 3(a)) are compared here. A rough surface with high density APBs is observed on standard Si (001), while in contrast GaAs on (111)-faceted Si (001) hollow structure exhibit an ultra-flat surface. This result experimentally proves the effectiveness of our designed structures for high quality III-V/Si hybrid growth.

Furthermore, a standard five-layer InAs/GaAs DWELLS structure is then grown on the GaAs/Si (001) substrate. Uniform InAs QDs on GaAs/Si are obtained with a density of $3.3 \times 10^{10} \text{ cm}^{-2}$ as AFM image shown in Figure 3(c), which indicates the high quality of GaAs film on (111)-faceted-sawtooth Si (001) hollow substrate.

Prior to the growth of InAs QD micropillars, a calibration growth of the gain region without DBRs was carried out. The room-temperature PL of the gain calibration sample is shown as the blue curve in Figure 4. By applying 15 (top) and 33.5 (bottom) pairs of DBRs to the InAs QD calibration sample, the

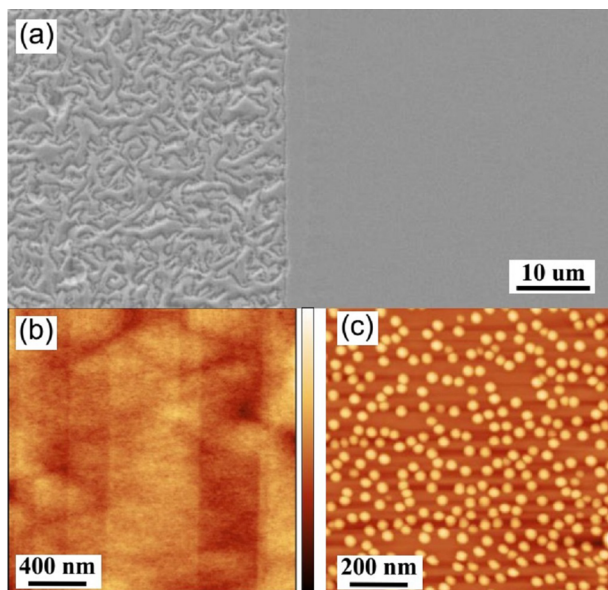


FIG. 3. (a) top-view SEM image of GaAs grown standard Si (001) and sawtooth-structured Si (001) substrates. (b) $2 \times 2 \mu\text{m}^2$ AFM image of the GaAs film grown on (111)-faceted-sawtooth Si (001) hollow substrate. (c) $1 \times 1 \mu\text{m}^2$ AFM image of InAs/GaAs QDs grown on GaAs/Si substrate.

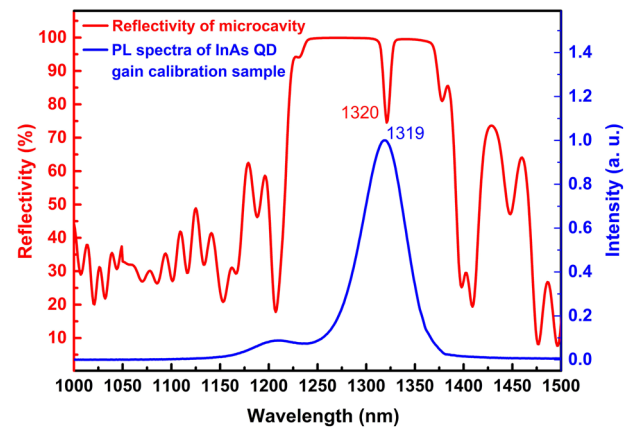


FIG. 4. Room-temperature PL spectra of InAs QD gain calibration sample (blue) and reflectivity (red) of InAs QD microcavity on Si (001) hollow substrate.

entire epi-structure for microcavity is formed. The measured reflectance stop-band of InAs QD microcavity on Si (001) is centered at $\sim 1300 \text{ nm}$ with corresponding bandwidth approximately 126 nm. The reflectivity at O-band wavelength is measured close to be 99.9% as shown in the red curve of Figure 4. To note, there is a subcavity resonance at 1320 nm from the reflectivity spectrum. The strong room-temperature PL of the Si-based InAs/GaAs QDs peaked at 1319 nm, which is in line with subcavity resonant wavelength. It is also to be noted that the reflectivity at 532 nm is 36.7%, which leads to the deducted pump power for L-L characterization of micropillars.

The laser operation of InAs QD micropillar cavities on Si (001) is identified by power dependent measurements at room temperature. The characterization of InAs QD micropillar lasers on Si (001) were performed on a micro-PL system with a continuous-wave (CW) pump laser at 532 nm. In this work, micropillar lasers with two different mesa sizes ($15 \mu\text{m}$ and $150 \mu\text{m}$) are characterized.

The laser characteristics (L-L curve) of InAs QD micropillar laser on Si substrate with mesa diameter of $15 \mu\text{m}$ is shown in Figure 5. Due to the relatively large size of micropillars, the devices are operating as multi-transverse mode lasers, which lead to the spectral broadening and asymmetry. Therefore, the collected output power here are calculated by integrating the spectrum of multiple laser modes. By linear fitting to the L-L curve, the laser threshold pump power is calculated as $20 \mu\text{W}$. The room-temperature spectral plot of micropillar laser with diameter of $15 \mu\text{m}$ at the pump power of 0.018 mW and 6 mW is shown in the inset of Figure 5, which exhibits significant linewidth narrowing from 17 nm to 1.3 nm by increasing the optical pump power. The InAs QD micropillar laser is peaked at 1320 nm, under the optical pump power of 6 mW. The relatively large FWHM is caused by the imperfection of circular mesa during patterning and etching process, which leads to the degradation in the quality factor of the microcavity.

In the case of pillar diameter of $150 \mu\text{m}$, the threshold pump power is determined to be approximately $680 \mu\text{W}$. The inset of Figure 6 plots the double logarithmic integrated

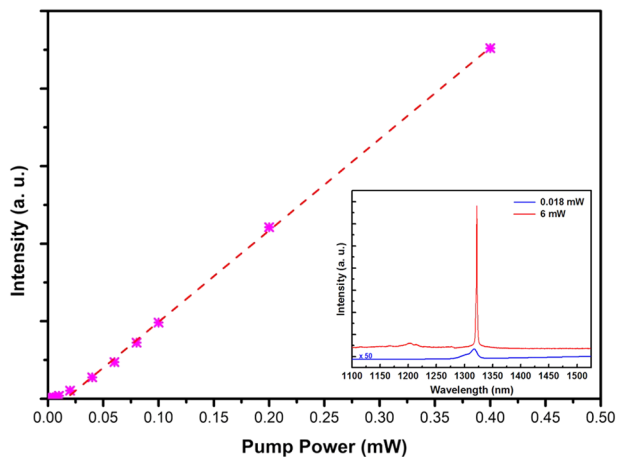


FIG. 5. Plot of output intensity versus pump power (L-L curve) of InAs/GaAs QD micropillar laser (diameter: 15 μm) on Si at room temperature. Inset: Spectral plot of micropillar laser with diameter of 15 μm at the pump power of 0.018 mW and 6 mW.

photoluminescence intensity versus pump power, revealing a typical “S-shaped” nonlinear transition from spontaneous emission to amplified spontaneous emission up to lasing.²⁶ The spontaneous emission coupling factor β will reduce significantly, when the optical microcavity increases the number of optical modes, which leads to significant reduction of threshold power.^{27,28}

In order to further investigate the performance of the devices, high-temperature operation of micropillar laser with mesa diameter of 150 μm are induced. Figure 7 shows the plot of integrated PL intensity of InAs QD micropillar with increasing pump power at different operating temperatures ranging from 20 $^{\circ}\text{C}$ to 100 $^{\circ}\text{C}$. To note, the measured results in Fig. 7

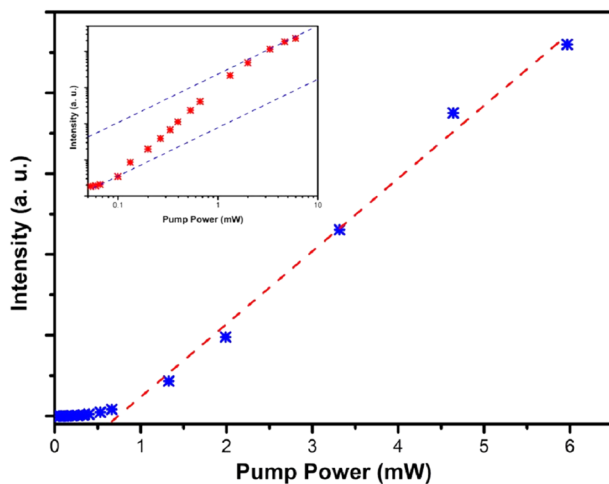


FIG. 6. Linear plot of light output versus pump power (L-L curve) of InAs/GaAs QD micropillar laser (diameter: 150 μm) on Si at room temperature. Inset: Double-log plot of the L-L curve.

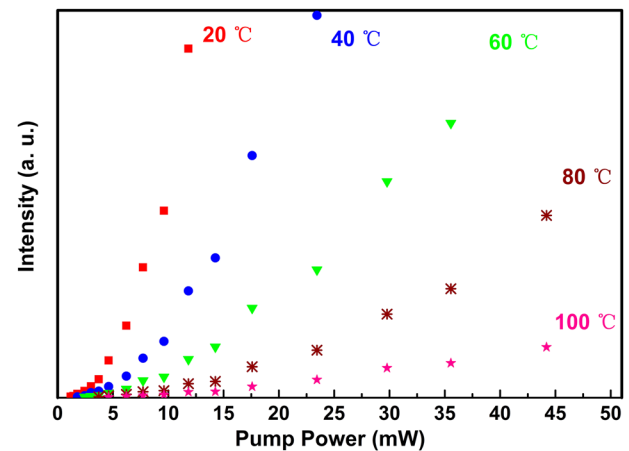


FIG. 7. Integrated PL intensity of InAs QD micropillar on Si (001) as a function of pump power at temperature ranging from 20 $^{\circ}\text{C}$ to 100 $^{\circ}\text{C}$.

are performed by different experimental arrangement, which consists of a high-power pump laser and proper thermal-electric cooling. Under the temperature-dependent L-L curve measurement, the high-power pump laser leads to a significant enlargement of beam spot size. Therefore, the effective pump power excited on the device is approximately 20% of values in Fig. 7.

During the experiment, the laser emission wavelength red-shifts linearly with increasing operation temperature by approximately 0.165 nm/ $^{\circ}\text{C}$. The results indicate the great temperature stability of InAs/GaAs QD microcavity lasers on Si (001) substrate, which verifies the capability of implementing (111)-faceted Si (001) hollow structure as a potential platform for III-V optoelectronic devices on standard Si (001) substrates.

IV. CONCLUSION

To summarize, we demonstrated a low threshold (20 μW) lasing of InAs/GaAs micropillar on (111)-faceted-sawtooth Si (001) hollow substrates using CMOS compatible techniques. The maximum operation temperature of the devices over 100 $^{\circ}\text{C}$ are achieved in this work. By implementing our in-situ hybrid growth method, high-quality III-V/Si (001) photonic structures could possibly be obtained on a 8-inch Si wafer with industrial 8-inch III-V MBE system. This technique represents an alternative approach of achieving high-yield and high-performance III-V/Si hybrid photonic devices for future silicon photonic on-chip integration.

ACKNOWLEDGMENTS

Financial support was provided by the National Natural Science Foundation of China (Grants 11504415, 11434010, 11574356 and 61635011), the National Key Research and Development Program of China (2016YFA0300600, 2016YFA0301700 and 2015CB932400), and the Key Research Program of Frontier Sciences, CAS (Grant No. QYZDB-SSW-JSC009). Ting Wang is

supported by the Youth Innovation Promotion Association of CAS (No. 2018011).

REFERENCES

- ¹V. R. Almeida, C. A. Barrios, R. R. Panepucci, and M. Lipson, "All-optical control of light on a silicon chip," *Nature* **431**(7012), 1081–1084 (2004).
- ²M. Asghari and A. V. Krishnamoorthy, "Silicon photonics: energy-efficient communication," *Nat. Photonics* **5**, 268–270 (2011).
- ³A. Rickman, "The commercialization of silicon photonics," *Nat. Photonics* **8**(8), 579–582 (2014).
- ⁴D. Liang and J. E. Bowers, "Recent progress in lasers on silicon," *Nat. Photonics* **4**(8), 511–517 (2010).
- ⁵S. Tanaka, S. H. Jeong, S. Sekiguchi, T. Kurahashi, Y. Tanaka, and K. Morito, "High-output-power, single wavelength silicon hybrid laser using precise flip-chip bonding technology," *Opt. Express* **20**(27), 28057–28069 (2012).
- ⁶Z. Zhou, B. Yin, and J. Michel, "On-chip light sources for silicon photonics," *Light Sci. Appl.* **4**(358), 1–13 (2015).
- ⁷T. Wang, H. Liu, A. Lee, F. Pozzi, and A. Seeds, "1.3- μm InAs/GaAs quantum-dot lasers monolithically grown on Si substrates," *Opt. Express* **19**(12), 11381–11386 (2011).
- ⁸S. M. Chen, M. C. Tang, J. Wu, Q. Jiang, V. G. Dorogan, M. Benamara, Y. I. Mazur, G. J. Salamo, A. J. Seeds, and H. Liu, "1.3 μm InAs/GaAs quantum-dot laser monolithically grown on Si substrates operating over 100 $^{\circ}\text{C}$," *Electron. Lett.* **50**(20), 1467–1468 (2014).
- ⁹S. M. Chen, W. Li, J. Wu, Q. Jiang, M. C. Tang, S. Shutts, S. N. Elliott, A. Sobiesierski, A. J. Seeds, I. Ross, P. M. Smowton, and H. Y. Liu, "Electrically pumped continuous-wave III-V quantum dot lasers on silicon," *Nat. Photonics* **10**(5), 307 (2016).
- ¹⁰J. Kwoen, B. Jang, J. Lee, T. Kageyama, K. Watanabe, and Y. Arakawa, "All MBE grown InAs/GaAs quantum dot lasers on on-axis Si (001)," *Opt. Express* **26**(9), 11568 (2018).
- ¹¹Y. H. Jhang, R. Mochida, K. Tanabe, K. Takemasa, M. Sugawara, S. Iwamoto, and Y. Arakawa, "Direct modulation of 1.3 μm quantum dot lasers on silicon at 60 $^{\circ}\text{C}$," *Opt. Express* **24**(16), 18428–18435 (2016).
- ¹²Y. T. Wan, Q. Li, A. Y. Liu, A. C. Gossard, J. E. Bowers, E. L. Hu, and K. M. Lau, "Optically pumped 1.3 μm room-temperature InAs quantum-dot micro-disk lasers directly grown on (001) silicon," *Opt. Express* **41**(7), 1664–1667 (2016).
- ¹³J. Norman, M. J. Kennedy, J. Selvidge, Q. Li, Y. Wan, A. Y. Liu, P. G. Callahan, M. P. Echlin, T. M. Pollock, K. M. Lau, A. C. Gossard, and J. E. Bowers, "Electrically pumped continuous wave quantum dot lasers epitaxially grown on patterned, on-axis (001) Si," *Opt. Express* **25**(4), 3927–3934 (2017).
- ¹⁴T. Wang, J. J. Zhang, and H. Liu, "Quantum dot lasers on silicon substrate for silicon photonic integration and their prospect," *Acta Physica Sinica* **64**, 204209 (2015).
- ¹⁵H. Liu, T. Wang, Q. Jiang, R. Hogg, F. Tutu, F. Pozzi, and A. Seeds, "Long-wavelength InAs/GaAs quantum-dot laser diode monolithically grown on Ge substrate," *Nat. Photonics* **5**, 416 (2011).
- ¹⁶Y. Wang, B. Wang, W. A. Sasangka, S. Bao, Y. Zhang, H. V. Demir, J. Michel, K. E. K. Lee, S. F. Yoon, E. A. Fitzgerald, C. S. Tan, and K. H. Lee, "High-performance ALGaInP light-emitting diodes integrated on silicon through a superior quality germanium-on-insulator," *Photon. Res.* **6**, 290 (2018).
- ¹⁷M. Martin, D. Caliste, R. Cipro, R. Alcotte, J. Moeyaert, S. David, F. Bassani, T. Cerba, Y. Bogumilowicz, E. Sanchez, Z. Ye, X. Y. Bao, J. B. Pin, T. Baron, and P. Pochet, "Toward the III-V/Si co-tegration by controlling the biatomic steps on hydrogenated Si (001)," *Appl. Phys. Lett.* **109**, 253103 (2016).
- ¹⁸Y. Wan, D. Jung, J. Norman, C. Shang, I. MacFarlane, Q. Li, M. J. Kennedy, A. C. Gossard, K. M. Lau, and J. E. Bowers, "O-band electrically injected quantum dot micro-ring lasers on on-axis (001) GaP/Si and V-groove Si," *Opt. Express* **25**(22), 26853–26860 (2017).
- ¹⁹D. Jung, P. G. Callahan, B. Shin, K. Mukherjee, A. C. Gossard, and J. E. Bowers, "Low threading dislocation density GaAs growth on on-axis GaP/Si (001)," *J. Appl. Phys.* **122**(22), 225703 (2017).
- ²⁰A. Y. Liu, J. Peters, X. Huang, D. Jung, J. Norman, M. L. Lee, A. C. Gossard, and J. E. Bowers, "Electrically pumped continuous-wave 1.3 μm quantum-dot lasers epitaxially grown on on-axis (001) GaP/Si," *Opt. Lett.* **42**(2), 338–341 (2017).
- ²¹M. Tang, S. Chen, J. Wu, Q. Jiang, V. G. Dorogan, M. Benamara, Y. I. Mazur, G. J. Salamo, A. Seeds, and H. Liu, "1.3- μm InAs/GaAs quantum-dot lasers monolithically grown on Si substrates using InAlAs/GaAs dislocation filter layers," *Opt. Express* **22**(10), 11528–11535 (2014).
- ²²A. Y. Liu, C. Zhang, A. Snyder, D. Lubyshev, J. M. Fastenau, A. W. K. Liu, A. C. Gossard, and J. E. Bowers, "MBE growth of P-doped 1.3 μm InAs quantum dot lasers on silicon," *J. Vac. Sci. Technol. B* **32**(2), 02C108 (2014).
- ²³Y. T. Wan, Q. Li, Y. Geng, B. Shi, and K. M. Lau, "InAs/GaAs quantum dots on GaAs-on-V-grooved-Si substrate with high optical quality in the 1.3 μm band," *Appl. Phys. Lett.* **107**(8), 081106 (2015).
- ²⁴B. Shi, S. Zhu, Q. Li, Y. T. Wan, E. L. Hu, and K. M. Lau, "Continuous-wave optically pumped 1.55 μm InAs/InAlGaAs quantum dot microdisk lasers epitaxially grown on silicon," *ACS Photonics* **4**(2), 204–210 (2017).
- ²⁵W. Q. Wei, J. H. Wang, B. Zhang, J. Y. Zhang, H. L. Wang, Q. Feng, H. X. Xu, and T. Wang, and J. J. Zhang, "InAs QDs on (111)-faceted Si (001) hollow substrates with strong emission at 1300 nm and 1550 nm," *Appl. Phys. Lett.* **113**, 103701 (2018).
- ²⁶S. M. Ulrich, C. Gies, S. Ates, J. Wiersig, S. Reitzenstein, C. Hofmann, A. Löffler, A. Forchel, F. Jahnke, and P. Michler, "Photon statistics of semiconductor microcavity lasers," *Phys. Rev. Lett.* **98**, 043906 (2007).
- ²⁷S. Reitzenstein, C. Hofmann, A. Gorbunov, M. Straub, S. H. Kwon, C. Schneider, A. Löffler, S. Hofling, M. Kamp, and A. Forchel, "AlAs/GaAs micropillar cavities with quality factors exceeding 150.000," *Appl. Phys. Lett.* **90**, 251109 (2007).
- ²⁸G. Shtengel, H. Temkin, T. Uchida, M. Kim, P. Brusenbach, and C. Parsons, "Spontaneous emission factor and its scaling in vertical cavity surface emitting lasers," *Appl. Phys. Lett.* **64**, 1062 (1994).